Fast & Accurate Far-Field Prediction by Using a Reduced Number of Bi-Polar Measurements

F. D'Agostino, F. Ferrara, C. Gennarelli, *Senior Member, IEEE,* R. Guerriero, M. Migliozzi

***Abstract*—This letter gives the experimental assessment of a near to far-field transformation (NTFFT) technique allowing the fast and accurate reconstruction of the antenna far field from a non-redundant, i.e. minimum, number of near-field (NF) data collected through a bi-polar scanning. Such a NTFFT relies on a non-redundant sampling representation of the voltage detected by the scanning probe, attained by shaping the antenna with an oblate ellipsoid, a model suitable to deal with quasi-planar antennas, as typically are the measured ones in a planar NF facility. The NF data necessary to execute the traditional plane-rectangular NTFFT are then effectively recovered from the acquired (non-redundant) bi-polar ones by exploiting a 2-D optimal sampling interpolation formula. This makes possible to achieve a remarkable acquisition time saving, which is a very relevant outcome, because this time is nowadays much greater than that needed to carry out the NTFFT.**

***Index Terms*—Antenna measurements, non-redundant sampling representations of electromagnetic fields, bi-polar near to far-field transformation.**

I. Introduction

The precise measurement of the radiation characteristics of an antenna can be achieved only in an anechoic chamber, where the free-space propagation conditions are very well reproduced, since the reflections from its walls, floor, and ceiling are almost completely suppressed. These accurate measurements are, f.i., required to verify the fulfillment of the design specifications in the case of high performance antennas. However, these last generally have a large extension with respect to the wavelength so that the far-field distance requirements cannot be satisfied, due to the limited sizes of an anechoic chamber, and, thus, only the near field radiated by them can be actually measured in it. In this case, the far field of the antenna under test (AUT) can be accurately recovered by applying near to far-field transformation (NTFFT) techniques [1, 2]. Among them, those wherein the near-field (NF) data are acquired on a plane, as in the plane-rectangular [3], plane-polar [4-7], and bi-polar [8-10] scans can be suitably adopted when testing high gain AUTs, which radiate pencil beam patterns and generally have a quasi-planar shape. From the analytical and computational viewpoints, the most simple and efficient one of the planar NTFFTs is that adopting the plane-rectangular scanning, since the AUT far field is effectively determined, through the 2-D fast Fourier transform (FFT), from the complex voltage NF data, detected by the probe and rotated probe on a plane-rectangular grid. The plane-polar NTFFT, as compared to the plane-rectangular one, offers the following advantages [4]: i) a simpler mechanical implementation, since it can be accomplished via rotary and linear motions of the AUT and probe, respectively; ii) a larger measurement zone for a given extent of the anechoic chamber; iii) a more accurate prediction of the far field of gravitationally sensitive spaceborne AUTs when the scanning is performed in a horizontal plane. The NTFFT using the bi-polar scanning (Fig. 1) is even more appealing, since it conserves all the advantages of that adopting the plane-polar one, while requiring a cheaper, simpler, and potentially more accurate NF measurement system. In fact, only rotary motions are used and, usually, rotary tables are more precise than linear positioners. Moreover, it has intrinsically the capability to maintain the planarity, since the arm is fixed to the rotary table at one of its ends and the AUT is attached to the other one, so that its bending is constant during the scan. By properly applying the non-redundant sampling representations of electromagnetic (EM) fields [11, 12] and assuming the AUT as contained in an oblate spheroid, 2-D optimal sampling interpolation (OSI) formulae, to get the voltage detected by the probe in its two orientations in the plane-rectangular grid needed to execute the traditional NTFFT [3] from a minimum number of its bi-polar samples, have been developed and numerically assessed in [10]. It is so possible to considerably lower the number of the needed NF measurements and acquisition time as compared to the techniques in [8, 9], which do not benefit from the non-redundant representations [11, 12].

The aim of this paper is just to give the experimental assessment of the non-redundant NTFFT with bi-polar scanning [10].

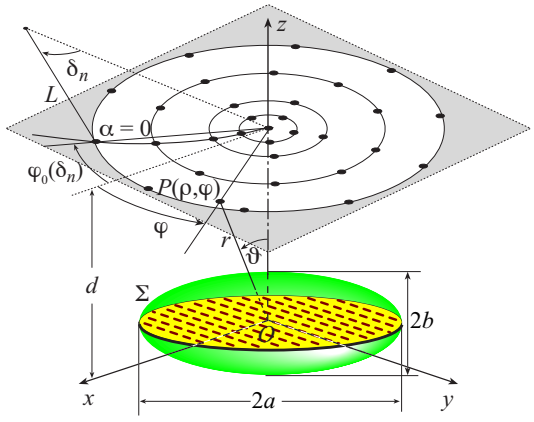

Fig. 1. Relevant to the bi-polar scanning.

Manuscript received July 17, 2017.

The authors are with the Department of Industrial Engineering, University of Salerno, 84084 Fisciano (SA), Italy (e-mail: cgennarelli@unisa.it).

II. Non-Redundant Voltage Representation

In this section, the non-redundant sampling representation of the voltage detected by a non-directive probe, that scans a plane at distance d from a quasi-planar AUT via a bi-polar NF measurement system, and the corresponding OSI formula are briefly recalled for the case wherein the AUT is considered as enclosed in an oblate spheroid [10]. The spherical coordinates (r, ϑ, φ) are used to specify any observation point, while the points lying on the plane can be also denoted by the bi-polar coordinates α and δ, which are the rotation angles of the AUT and arm, respectively (Fig. 1). It is very easy to verify that the bi-polar coordinates (α, δ) are mapped into the polar ones (ρ, φ) by:

$$(\rho,\varphi) = (2L\sin(\delta/2), \alpha - \delta/2) \tag{1}$$

L being the length of the bi-polar arm.

The non-redundant representations [11] can be profitably exploited for representing the voltage detected by the considered probe, since its spatial bandwidth practically coincides with the AUT radiated field one. Moreover, because the arcs traced by the arm are not meridian curves, it is opportune, as in the plane-polar scanning, to describe the plane through diameters and rings. Therefore, once the smallest oblate spheroid having major and minor axes equal to $2a$ and $2b$ has been chosen as surface Σ enclosing the AUT, an optimal parameter ξ must be used to describe these curves and a suitable phase factor $e^{-j\gamma(\xi)}$ has to be extracted from the voltage V_α or V_δ detected by the probe in its two orientations, probe/rotated probe (Fig. 2). The so obtained "reduced voltages" $\tilde{V}_{\alpha,\delta}(\xi) = V_{\alpha,\delta}(\xi)e^{j\gamma(\xi)}$ are not strictly spatially bandlimited functions, thus an error arises when approximating them by bandlimited functions. Such an error can be made reasonably small as the bandwidth is greater than a critical value W_ξ [11] and successfully reduced by considering an increased bandwidth $\chi' W_\xi$, where χ' is an enlargement bandwidth factor a bit greater than one for AUTs with large sizes in terms of wavelengths [11].

When considering a diameter, the bandwidth W_ξ, the optimal parameter ξ and the related phase function γ are [10, 11]:

$$W_\xi = \frac{4a}{\lambda}E(\pi/2|\sigma^2)\ ;\quad \xi = \frac{\pi}{2}\left[E\left(\sin^{-1}u|\sigma^2\right)\Big/E\left(\pi/2|\sigma^2\right)\right] \tag{2}$$

$$\gamma = \frac{2\pi a}{\lambda}\left[v\sqrt{\frac{v^2-1}{v^2-\sigma^2}} - E\left(\cos^{-1}\sqrt{\frac{1-\sigma^2}{v^2-\sigma^2}}\,\Big|\,\sigma^2\right)\right] \tag{3}$$

wherein $E(\bullet\,|\,\bullet)$ is the second kind elliptic integral, λ is the free-space wavelength, $\sigma = f/a$ is the ellipsoid eccentricity, $2f$ the interfocal distance, and $u = (r_1 - r_2)/2f$, $v = (r_1 + r_2)/2a$ are the elliptic coordinates, with $r_{1,2}$ being the distances from the foci to the observation point P.

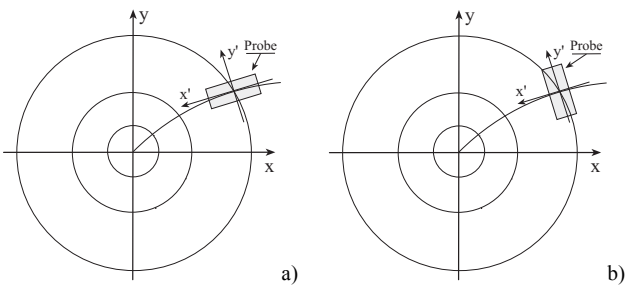

Fig. 2. a) measurement of V_α , b) measurement of V_δ.

The optimal parameter ξ for describing a ring is the angle φ, the phase function is constant, and the related bandwidth [10, 11] becomes $W_\varphi(\xi) = (2\pi a/\lambda)\sin\vartheta_\infty(\xi)$, wherein $\vartheta_\infty = \sin^{-1}u$ is the angle between the z axis and the asymptote to the hyperbola passing through P.

The voltages V_α and V_δ can be accurately determined at all points $P(\rho, \varphi)$ on the scanning plane and, thus, also at those belonging to the grid of the classical plane-rectangular NTFFT [3] via the following 2-D OSI formula [10]:

$$V_{\alpha,\delta}\left(\xi(\rho),\varphi\right) = e^{-j\gamma(\xi)}\sum_{n=n_0-q+1}^{n_0+q}\left\{G(\xi,\xi_n,\bar{\xi},N,N'')\cdot \sum_{m=m_0-p+1}^{m_0+p}\tilde{V}_{\alpha,\delta}(\xi_n,\varphi_{m,n})\,G(\varphi,\varphi_{m,n},\bar{\varphi}_n,M_n,M_n'')\right\} \tag{4}$$

where $n_0 = \lfloor \xi/\Delta\xi \rfloor$, $m_0 = \lfloor (\varphi - \varphi_0(\xi_n))/\Delta\varphi_n \rfloor$, $2q$ and $2p$ are the numbers of the considered nearest reduced voltage samples,

$$\xi_n = 2\pi n/(2N''+1) = n\Delta\xi\ ;\quad N'' = \lfloor \chi N' \rfloor + 1 \tag{5}$$

$$N' = \lfloor \chi' W_\xi \rfloor + 1\ ;\quad \bar{\xi} = q\Delta\xi\ ;\quad N = N'' - N' \tag{6}$$

$$\varphi_{m,n} = \varphi_0(\xi_n) + m\Delta\varphi_n = -\delta_n/2 + 2\pi m/(2M_n''+1) \tag{7}$$

$$M_n'' = \lfloor \chi M_n' \rfloor + 1\ ;\ M_n' = \lfloor \chi^* W_\varphi(\xi_n) \rfloor + 1\ ;\ M_n = M_n'' - M_n' \tag{8}$$

$$\bar{\varphi}_n = p\Delta\varphi_n;\quad \chi^* = 1 + (\chi' - 1)\left[\sin\vartheta_\infty(\xi_n)\right]^{-2/3} \tag{9}$$

$\lfloor x \rfloor$ being the integer part of x and $\chi > 1$ an oversampling factor required for the control of the truncation error [11]. In (4)

$$G(\eta,\eta_k,\bar{\eta},J,J'') = \Omega_J(\eta - \eta_k,\bar{\eta})\,D_{J''}(\eta - \eta_k) \tag{10}$$

is the OSI interpolation function, wherein

$$\Omega_J(\eta,\bar{\eta}) = \frac{T_J\left[2\cos^2(\eta/2)\big/\cos^2(\bar{\eta}/2) - 1\right]}{T_J\left[2\big/\cos^2(\bar{\eta}/2) - 1\right]} \tag{11}$$

$$D_{J''}(\eta) = \frac{\sin\left[(2J''+1)\,\eta/2\right]}{(2J''+1)\sin(\eta/2)} \tag{12}$$

are the Tschebyscheff and Dirichlet sampling functions [11], $T_J(\eta)$ being the Tschebyscheff polynomial of degree J.

The 2-D OSI formula (4) is similar to that developed in the case of the plane-polar scanning, the only difference is due to the fact that, as a consequence of the bi-polar arm rotation (see Fig. 1), each sample lying on the n-th ring is shifted with respect to the related plane-polar one by $\varphi_0(\xi_n) = -\delta_n/2$.

As regards the AUT FF reconstruction, it must be stressed that the probe corrected formulae in [3] (which in the here used reference system can be recast as in [6, 13]) hold only when the axes of the probe and AUT remain parallels during the scan and this implies that the probe has to co-rotate with the AUT. To avoid this co-rotation, a probe having a first-order azimuthal dependence in its FF pattern must be used. In this case,

the voltages collected with co-rotation by the probe and rotated probe, say V_y and V_x, are determined from the knowledge of V_α and V_δ by the following software co-rotation formulae:

$$V_y = V_\alpha \cos(\varphi - \delta/2) - V_\delta \sin(\varphi - \delta/2) \qquad (13)$$

$$V_x = V_\alpha \sin(\varphi - \delta/2) + V_\delta \cos(\varphi - \delta/2) \qquad (14)$$

To this end, an open-ended rectangular waveguide can be profitably used as probe, instead of the open-ended circular one considered in [10]. In fact, when excited by a TE_{10} mode, its radiated far field in the forward hemisphere has an azimuthal dependence that can be well approximated by a first-order one [14].

III. Experimental Testing

The experimental tests have been performed at the Antenna Characterization Lab of the University of Salerno, where it is available an anechoic chamber $8\text{m}\times5\text{m}\times4\text{m}$ sized and covered by pyramidal absorbers, which guarantee a reflectivity level smaller than – 40 dB. It is provided with a NF measurement system that allows spherical, cylindrical, and plane-polar scannings, as well as those along the related spirals. The plane-polar scanning is realized by attaching the probe to a vertical slide and mounting the AUT on a rotary table having its axis orthogonal to the linear positioner. An additional rotary table, placed between this positioner and the probe, allows to employ the plane-polar NF facility to acquire the NF data which would be measured by both plane-rectangular and bi-polar NF measurement systems. This table enables also the measurement of the NF data which would be collected in a bi-polar NF facility with hardware co-rotation, wherein the axes of the probe and AUT are kept parallel during the scanning. A vector network analyzer is employed to perform the measurement of amplitude and phase of the voltage detected by the probe, an open-ended WR-90 rectangular waveguide. The AUT is an E-plane monopulse antenna working at 10 GHz in the sum mode. It has been made by a hybrid Tee and two pyramidal horns with the apertures placed in the plane *xy* of the reference system. The horns apertures have sizes $8.9\text{cm}\times6.8\text{cm}$ and the distance between their centers is 26.5 cm. An oblate spheroid with $2a = 37.2$ cm and $2b = 16.6$ cm has been employed to model this AUT.

The non-redundant bi-polar NF samples have been acquired in a circle with diameter 210 cm on a plane 16.5 cm away from the AUT, in correspondence of the points fixed by the presented non-redundant sampling representation in the case of $L = 120$ cm, $\chi' = 1.35$, and $\chi = 1.25$. The amplitude and phase of V_α reconstructed on the diameter at $\varphi = 0°$ from the non-redundant bi-polar samples are compared in Figs. 3 and 4 with those directly acquired. The reconstruction of the amplitude of V_α on the diameter at $\varphi = 45°$ is shown in Fig. 5, while the corresponding one relevant to V_δ is displayed in Fig. 6. As can be noticed, all recovered patterns are very accurate, except for small discrepancies in the zones where the voltage level is very low, thus assessing the effectiveness of the 2-D OSI formula. It is worthy to note that the recovered patterns show a smoother behavior than the measured ones, since the spectral content of the noise at the spatial frequencies higher than the spatial bandwidth of the antenna are cut away owing to the low pass filtering characteristics of the employed interpolation function. Finally, the overall efficacy of this NTFFT is validated by comparing the FF patterns in the principal planes (Figs. 7 and 8) reconstructed from the non-redundant bi-polar measurements with the reference patterns got from the plane-rectangular ones directly acquired, at 0.45λ spacing, on the $140\text{cm}\times140\text{cm}$ inscribed square. As can be seen, a very good agreement is found in the E-plane, while a less accurate reconstruction can be observed in the H-plane. This is due to the fact that the far field of an open-ended rectangular waveguide excited by the fundamental mode TE_{10} shows only approximately a first-order azimuthal dependence [14], which, indeed, is shown by an open-ended circular waveguide excited by the TE_{11} mode. The FF reconstruction got from the acquired non-redundant bi-polar NF

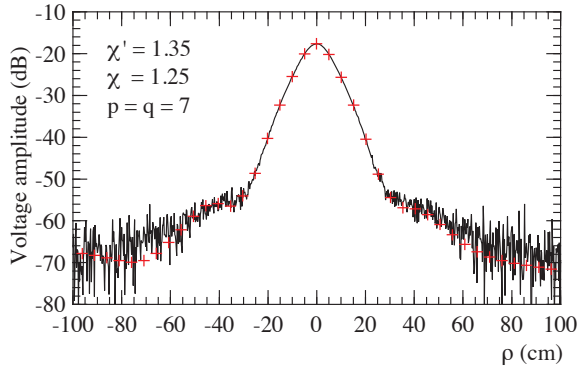

Fig. 3. Amplitude of V_α on the diameter at $\varphi = 0°$. —— measured. + + + interpolated from the non-redundant bi-polar NF samples.

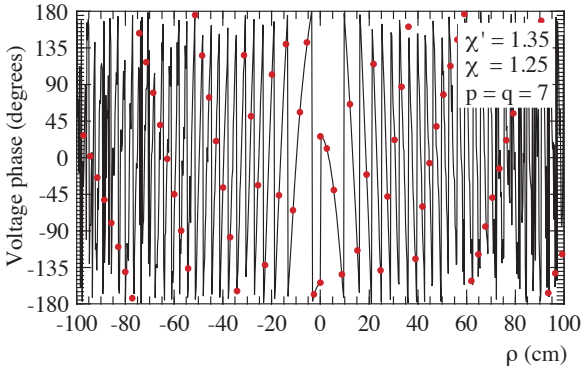

Fig.4 . Phase of V_α on the diameter at $\varphi = 0°$. —— measured. • • • • interpolated from the non-redundant bi-polar NF samples.

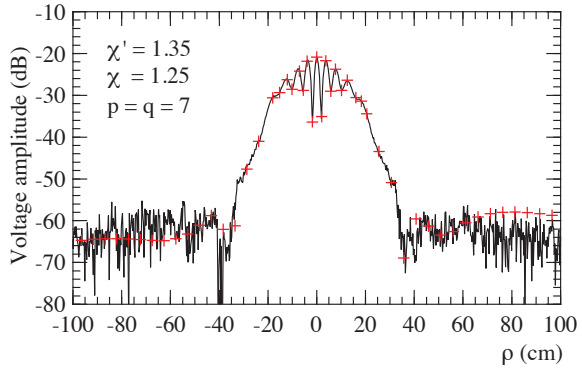

Fig. 5. Amplitude of V_α on the diameter at $\varphi = 45°$. —— measured. + + + interpolated from the non-redundant bi-polar NF samples.

samples when using the hardware co-rotation results to be very accurate also in the H-plane (Fig. 9). It must be stressed that the used non-redundant bi-polar NF samples are 1836 and, thus, remarkably less than those (18631) required by the bi-polar scanning techniques [8, 9] to cover the same measurement area.

Further experimental results, validating the effectiveness of the described NTFFT technique and relevant to a different AUT, have been shown in [15].

IV. Conclusion

The validity of the non-redundant bi-polar NTFFT using an oblate spheroid to shape the AUT has been experimentally investigated. The very good NF and FF reconstructions obtained in the laboratory testing have fully proved its effectiveness also from a practical viewpoint. In particular, it has been shown that it allows to precisely predict the AUT far field from a minimum number of bi-polar NF samples, thus remarkably saving the acquisition time as compared to the previous techniques [8, 9].

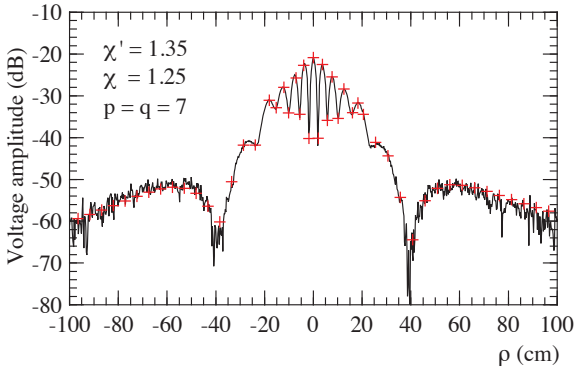

Fig. 6. Amplitude of V_δ on the diameter at $\varphi = 45°$. ——— measured. + + + interpolated from the non-redundant bi-polar NF samples.

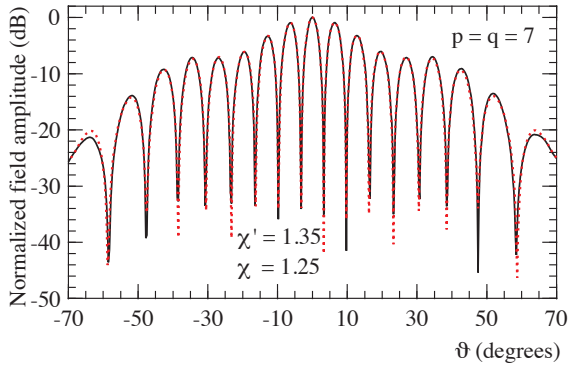

Fig. 7. E-plane pattern. ——— reference. – – – recovered from the non-redundant bi-polar NF samples with software co-rotation.

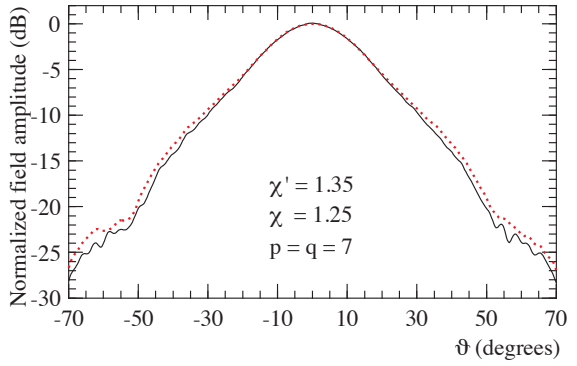

Fig. 8. H-plane pattern. ——— reference. – – – recovered from the non-redundant bi-polar NF samples with software co-rotation.

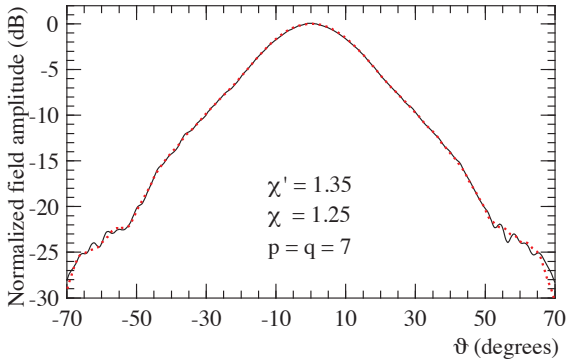

Fig. 9. H-plane pattern. ——— reference. – – – recovered from the non-redundant bi-polar NF samples with hardware co-rotation.

References

[1] A.D. Yaghjian, "An overview of near-field antenna measurements," *IEEE Trans. Antennas Propag.*, vol. AP-34, no. 1, pp. 30-45, Jan. 1986.

[2] F. Ferrara, C. Gennarelli, and R. Guerriero, "Near-field antenna measurement techniques," in *Handbook of Antenna Technologies*, Z.N. Chen, D. Liu, H. Nakano, X. Qing, and T. Zwick, Eds., Singapore: Springer, 2016.

[3] E.B. Joy, W.M. Leach, Jr., G. P. Rodrigue and D.T. Paris, "Application of probe-compensated near-field measurements," *IEEE Trans. Antennas Propag.*, vol. AP-26, no. 3, pp. 379-389, May 1978.

[4] Y. Rahmat-Samii, V. Galindo Israel, and R. Mittra, "A plane-polar approach for far-field construction from near-field measurements," *IEEE Trans. Antennas Propag.*, vol. AP-28, no. 2, pp. 216-230, March 1980.

[5] M.S. Gatti and Y. Rahmat-Samii, "FFT applications to plane-polar near-field antenna measurements," *IEEE Trans. Antennas Propag.*, vol. 36, no. 6, pp. 781-791, June 1988.

[6] F. D'Agostino, F. Ferrara, C. Gennarelli, R. Guerriero, and M. Migliozzi, "Reconstruction of the antenna far-field pattern through a fast plane-polar scanning," *Appl. Comp. Electr. Soc. J.*, vol. 31, no. 12, pp. 1362-1369, Dec. 2016.

[7] F. D'Agostino, F. Ferrara, C. Gennarelli, R. Guerriero, and M. Migliozzi, "Far-field pattern reconstruction from a nonredundant plane-polar near-field sampling arrangement: experimental testing," *IEEE Antennas Wireless Propag. Lett.*, vol. 15, pp. 1345-1348, 2016.

[8] L.I. Williams, Y. Rahmat-Samii, and R.G. Yaccarino, "The bi-polar planar near-field measurement technique, Part I: implementation and measurement comparisons," *IEEE Trans. Antennas Propag.*, vol. 42, no. 2, pp. 184-195, Feb. 1994.

[9] R.G. Yaccarino, Y. Rahmat-Samii, and L.I. Williams, "The bi-polar near-field measurement technique, Part II: near-field to far-field transformation and holographic imaging methods," *IEEE Trans. Antennas Propag.*, vol. 42, no. 2, pp. 196-204, Feb. 1994.

[10] F. D'Agostino, C. Gennarelli, G. Riccio, and C. Savarese, "Data reduction in the NF-FF transformation with bi-polar scanning," *Microw. Optic. Technol. Lett.*, vol. 36, no. 1, pp. 32-36, Jan. 2003.

[11] O.M. Bucci, C. Gennarelli, and C. Savarese, "Representation of electromagnetic fields over arbitrary surfaces by a finite and nonredundant number of samples," *IEEE Trans. Antennas Propag.*, vol. 46, no. 3, pp. 351-359, Mar. 1998.

[12] O.M. Bucci and C. Gennarelli, "Application of nonredundant sampling representations of electromagnetic fields to NF-FF transformation techniques," *Int. J. Antennas Propag.*, vol. 2012, ID 319856, 14 pages, 2012.

[13] F. D'Agostino, F. Ferrara, C. Gennarelli, R. Guerriero, S. McBride, and M. Migliozzi, "Fast and accurate antenna pattern evaluation from near-field data acquired via planar spiral scanning," *IEEE Trans. Antennas Propag.*, vol. 64, no. 8, pp. 3450-3458, Aug. 2016.

[14] A.D. Yaghjian, "Approximate formulas for the far field and gain of open-ended rectangular waveguide," *IEEE Trans. Antennas Propag.*, vol. AP-32, no. 4, pp. 378-384, Apr.1984.

[15] F. D'Agostino, F. Ferrara, C. Gennarelli, R. Guerriero, and M. Migliozzi, "Nonredundant NF-FF transformation with bi-polar scanning: experimental testing," in *Proc. Antenna Meas. Tech. Ass.*, pp. 212-217, 2016.